JOURNAL OF MATERIALS SCIENCE 29 (1994) 5165–5176

Microsphere-filled lightweight calcium phosphate cements

TOSHIFUMI SUGAMA
Energy Efficiency and Conservation Division, Department of Applied Science, Brookhaven National Laboratory, Upton, NY 11973, USA

E. WETZEL
University of Delaware, Department of Mechanical Engineering, Newark, DE 19716, USA

The incorporation of inorganic and organic microsphere fillers into calcium phosphate cement (CPC) to produce lightweight cementitious materials that could be used under hydrothermal conditions at high temperatures between 200 and 1000 °C was investigated. An aluminosilicate based hollow microsphere, with a density of 0.67 g cm^{-3} and a particle size of 75–200 μm, was the most suitable having a low slurry density of ≈1.3 g cm^{-3}, and a compressive strength greater than 6.89 MPa. This microsphere-filled lightweight CPC exhibited the following characteristics: 1. after autoclaving at 200 °C, amorphous ammonium calcium orthophosphate (AmCOP) salt and $Al_2O_3 \cdot xH_2O$ gel phases, formed by the reaction between calcium aluminate cement and an $NH_4H_2PO_4$ based fertilizer, were primarily responsible for the development of strength; 2. at a hydrothermal temperature of 300 °C, the microsphere shell moderately reacted with the CPC to form an intermediate reaction product, epistilbite (EP), while crystalline hydroxyapatite (HOAp) and boehmite (BO) were yielded by the phase transformations of AmCOP and $Al_2O_3 \cdot xH_2O$, respectively; 3. at an annealing temperature of 600 °C, the HOAp phase remained in the cement body, even though an EP → anorthite (AN) phase transition occurred; 4. at 1000 °C, the phase conversion of HOAp into whitlockite was completed, while the AN phase was eliminated; and 5. the microsphere demonstrated excellent thermal stability up to temperatures of 1000 °C.

1. Introduction

The attack of CO_2-containing brine on conventional cements in geothermal wells at temperatures up to 300 °C significantly shortens their service life [1, 2]. Na_2CO_3-related carbonation causes dissolution of cement which is converted into water-soluble salts, and also causes the severe corrosion of steel pipes, thereby resulting in the total disruption of the cement-supported well structure. Alkaline carbonation of the cement can be avoided by replacing the conventional geothermal cements with phosphate-bonded cements, such as calcium [3] and aluminium phosphate compounds [4]. Such phosphate cements are hydrothermally synthesized through an acid–base reaction, using calcium aluminate cements or aluminas as the base reactants, and ammonium dihydrogenphosphate based fertilizers as the acid reactant. Although some carbonation of hydroxyapatite, $Ca_5(PO_4)_3(OH)$, formed by the hydrothermally catalysed transformation of amorphous ammonium calcium orthophosphate, $NH_4CaPO_4 \cdot xH_2O$, occurs from an exchange reaction between CO_2 and the OH^- in hydroxyapatite [5], its rate is very slow compared with those of other cement systems, such as calcium aluminate, API class G, and class H. Further, after exposure to a Na_2CO_3 laden solution for six months at 200 °C, the calcium phosphate cement (CPC) specimens still maintain a compressive strength of >20 MPa. Such promising results encouraged the development of formulations for CPC based material systems which can be used to complete geothermal wells. The use of cementing slurries of normal density, 1.9–2.0 g cm^{-3}, for completing geothermal wells frequently results in problems of lost circulation when attempts are made to cement the well in weak unconsolidated rock zones with very fragile gradients. These unconsolidated formations fracture from the significant hydrostatic pressures required to pump the highly dense cement slurries. To avoid this problem, low density cement slurries are needed.

There are two means of preparing lightweight hydraulic cement slurries: one method is to introduce air bubbles into the slurry, and the other is to incorporate pressure-resistant hollow microspheres into the

* This work was performed under the auspices of the US Department of Energy, Washington, DC, under Contract No. DE-AC02-76CH00016.

0022–2461

cement slurry. It was reported [6] that the adherence of hollow beads to hydraulic cement matrices is one important factor which enhanced the cement's effectiveness in controlling problems of lost circulation. The treatment of sillimanite based microspheres with hot $Ca(OH)_2$ significantly increased the strength of the interfacial cement–sphere bond, which is responsible for the development of strength in ordinary autoclaved lightweight cements. This increase is due to the cross-linking and coupling of Ca-rich epitaxial layers formed by interaction between the $Ca(OH)_2$ and microspheres.

The objective of this research was to assess the viability of using commercial inorganic and organic microspheres as lightweight fillers of CPC. These hollow microspheres were evaluated mainly on the relationship between the densities of the slurries and compressive strengths of various microsphere-filled lightweight CPC (LCPC) specimens. Although geothermal cements are commonly used at hydrothermal service temperatures up to only 300 °C, the changes in strength of the 300 °C autoclaved CPC specimens after exposure in air at 600 and 1000 °C were also investigated. The mechanical behaviour of the lightweight CPC specimens prepared over this wide temperature range were then correlated with the phase compositions, transformations and morphological features of the composite cement matrices, and also with the chemical elements and microstructural developments at the contact zones near the microsphere particles which provided information on the possible interaction mechanism between the CPC and microspheres.

2. Experimental procedure

2.1. Materials

The calcium aluminate cement used as the Ca cation-liberating base reactant was SECAR 80 (No. 80), supplied by Lafarge Calcium Aluminates. The typical components of the No. 80 cement are 79.5–81.5 wt % Al_2O_3, 17.5–19.5 wt % CaO, < 0.1 wt % TiO_2, < 0.4 wt % SiO_2, < 0.25 wt % Fe_2O_3, < 0.2 wt % MgO, < 0.7 wt % $K_2O + Na_2O$ and < 0.2 wt % SO_3. X-ray powder diffraction (XRD) showed that the major phases of the cement are monocalcium aluminate, $CaO \cdot Al_2O_3$ (CA) and calcium dialuminate, $CaO \cdot 2Al_2O_3$, (CA_2). An ammonium polyphosphate fertilizer solution, known commercially as Poly-N (fertilizer grade: 11–37–0), was employed as the proton-donating acid liquid reactant. The chemical composition of Poly-N is 11.1 wt % ammoniacal N, 37.0 wt % P_2O_5, 0.16 wt % Fe, 0.11 wt % MgO, 0.12 wt % Al_2O_3, 0.12 wt % F, 0.6 wt % S and 50.79 wt % water. XRD and infrared (i.r.) analyses of Poly-N solid dried at 120 °C showed that its major component is ammonium dihydrogen monobasic orthophosphate (AmDHOP), $NH_4H_2PO_4$.

Five commercial inorganic and organic microspheres, Q-Cel 650 (Q-C, PQ Corp.), Extendospheres (EX, PQ Corp.), Macrolite (MA, 3M Corp.), Glass Bubbles (GL, 3M Corp.) and Dualite M6017AE (DU, Pierce & Stevens Corp.), were incorporated into the CPC as lightweight fillers. Q-C, EX, GL and DU microspheres are hollow, while MA is categorized as non-hollow. The shells of all of the spheres, except the polymeric DU sphere, are made of inorganic materials.

Table I shows the formulations of the microsphere-filled LCPC slurries. For 30 min, after the chemical components of the LCPC slurry systems were thoroughly mixed, numerous bubbles of NH_3 gas evolved. To avoid errors caused by bubbles trapped in the slurry, the densities of the slurries were measured at room temperature 1 h after mixing. Table I shows the densities of the LCPC slurries ranged from 1.55 to 1.18 g cm^{-3}, while the untreated CPC slurry had a density of 1.98 g cm^{-3}.

TABLE I Formulation and density of microsphere-filled lightweight CPC slurry systems

Sample No.	Compositions (vol %)							Slurry density (g cm^{-3})
	No. 80	Poly-N	Q-C	EX	MA	GL	DU	
C	30.6	69.4	–	–	–	–	–	1.98
C-1-1	18.9	50.1	31.0	–	–	–	–	1.37
C-1-2	16.0	48.6	35.4	–	–	–	–	1.32
C-1-3	11.6	43.9	44.5	–	–	–	–	1.18
C-2-1	18.9	50.2	–	30.9	–	–	–	1.50
C-2-2	14.5	43.9	–	41.6	–	–	–	1.32
C-2-3	9.9	45.2	–	44.9	–	–	–	1.22
C-3-1	17.9	54.4	–	–	27.7	–	–	1.55
C-3-2	13.0	55.5	–	–	31.5	–	–	1.44
C-3-3	10.0	56.9	–	–	33.1	–	–	1.34
C-4-1	18.8	53.3	–	–	–	27.9	–	1.47
C-4-2	15.9	48.4	–	–	–	35.7	–	1.32
C-4-3	13.0	44.4	–	-	–	42.6	–	1.20
C-5-1	24.4	55.5	–	–	–	–	20.1	1.55
C-5-2	22.1	50.3	–	–	–	–	27.6	1.36
C-5-3	20.2	45.9	–	–	–	–	33.9	1.28

The LCPC specimens for strength tests were prepared first by dry-mixing the CAC powder with the filler; Poly-N was added and the slurry was thoroughly hand-mixed for ≈3 min. Next, the LCPC slurry was cast into cylindrical moulds 30 mm in diameter and 65 mm high and cured at room temperature for ≈2 h. The slurries then were autoclaved at 200 or at 300 °C for 20 h. Other specimens were autoclaved at 300 °C for 20 h and then heated in an oven at 600 or 1000 °C for 16 h.

2.2. Measurements

The properties of the various microspheres, namely bulk density, particle size and chemical composition, were measured using helium comparison pycnometry, scanning electron microscopy (SEM), and X-ray photoelectron spectroscopy (XPS), respectively. Tests of compressive strength were performed on the LCPC cylinders; the results given are the average value of three specimens. The phase compositions and transformations of the LCPCs after heating in the autoclave and in the oven at temperatures up to 1000 °C were explored using X-ray powder diffraction (XRD) and Fourier transform infrared (FTIR) spectroscopy. An image analysis using SEM coupled with energy dispersion X-ray spectrometry (EDX) was made of the LCPC fracture surface to determine its microstructure and also the chemical components in the matrix and in the critical contact zones between the CPC and microspheres.

3. Results and discussion

3.1. Properties of microspheres

Fig. 1 shows a typical SEM micrograph of the "as-received" inorganic microspheres. Q-C microspheres

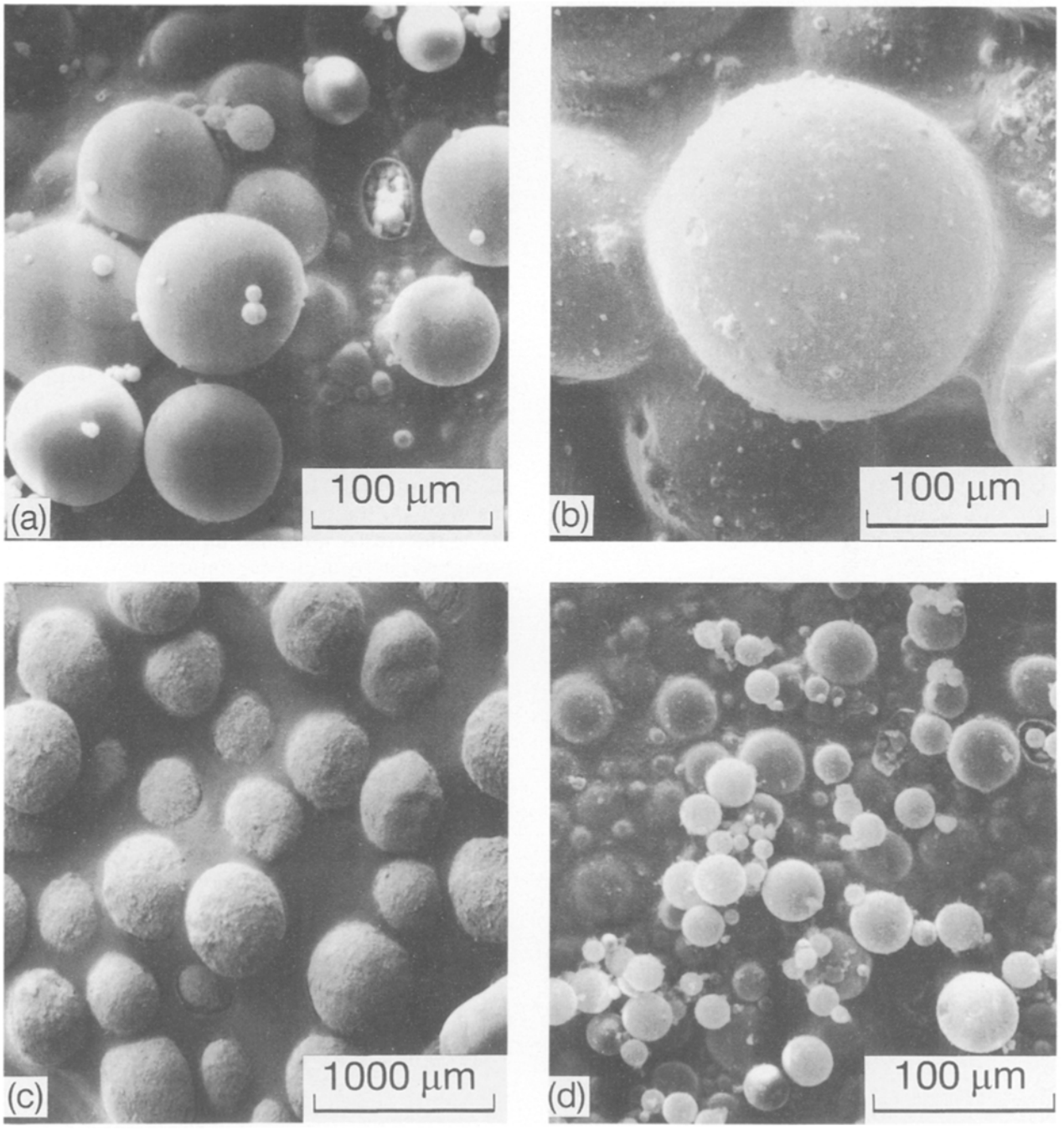

Figure 1 SEM micrographs of "as-received" microsphere surfaces: (a) Q-C, (b) EX, (c) MA and (d) GL.

(left, top) vary in size from ≈6 to ≈95 μm, and their shell surfaces are smooth. In contrast, a rough surface was observed on the EX microspheres (right, top), whose particle size ranged from ≈75 to ≈200 μm. The largest spheres, ranging from ≈300 to ≈450 μm, were MA (left, bottom). GL microspheres (right, bottom) were smooth and had the finest sizes, 5–45 μm. In comparison to SEM images of these ceramic microspheres, the surface of the microspheres of the acrylonitrile copolymer, DU, displayed a unique morphology (Fig. 2). The polymer surfaces were coated uniformly with a powdery material. EDX analysis of this substance at the location denoted as "a" revealed a large amount of Ca. To identify Ca based sizing material, the DU microspheres were inspected by XRD. The resulting data (not shown) indicated the formation of calcite, $CaCO_3$, as the sizing layer over the copolymer shell. Also, as seen in the SEM images, the surface indentations of some DU spheres reflected the elastic behaviour of the polymer shells.

The properties of the microspheres, such as density, particle size and surface chemical compositions are summarized in Table II. MA microspheres had the highest density of 1.25 g cm^{-3}, while the $CaCO_3$ modified DU microspheres had the lowest density, 0.13 g cm^{-3}. The other densities ranged from 0.67 to 0.38 g cm^{-3}. The surface chemical composition of Q-C inspected by XPS consisted of 11.0% Si, 21.3% B, 15.2% C, 2.3% K, 37.7% O and 12.5% Na. According to the material safety data sheet from PQ Corp., these elements compose an organosilicon modified soda-borosilicate glass containing some K. Although the manufacturer's data sheet stated that EX contains aluminosilicate, compounds comprised of Al, Si, O and C were the predominant elements, with a small amount of K and Na. C may have been an atmospheric contaminant or may have been introduced during manufacture. The non-hollow MA microspheres consist of multiple elements, Si, Al, C, K, O, Fe and Na. Except for C and Fe, these elements may reflect the presence of nepheline syenite, $KNa_3Al_4Si_4O_{16}$, which was identified by the 3M Corporation. The surface composition of the GL microsphere was similar to that of Q-C, differing only in the incorporation of Ca. Information from 3M indicated that this composition corresponds to soda-lime-borosilicate glass. The surfaces of the acrylonitrile DU shells revealed a large amount of Ca, due to the $CaCO_3$ sizing material. No Si, Al, B, K or Na was found on this surface.

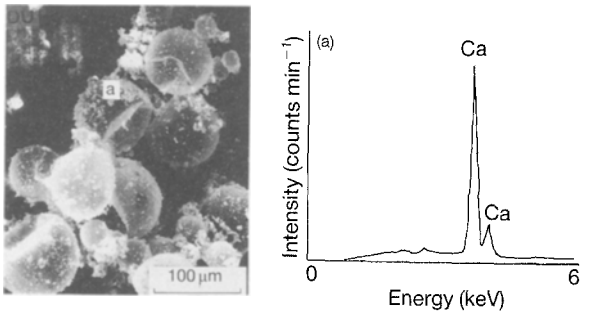

Figure 2 SEM–EDX inspection of $CaCO_3$ coated DU microspheres.

3.2. Compressive strength

Fig. 3 shows the changes in compressive strength for the various LCPC specimens as a function of slurry density. The specimens were autoclaved for 20 h at 200 or 300 °C, or autoclaved at 300 °C and heated in air in an oven for 16 h at 600 or 1000 °C. For the 200 °C autoclaved specimens, the compressive strengths of the cements depended mainly on the density of the original slurry and the species of microsphere filler. The strengths of all the various lightweight specimens tended to drop with decreasing density of the slurry. For the middle range density of ≈1.35 g cm^{-3}, LCPC strengths were in this order: EX > Q-C = GL > DU > MA. The poor performance of the MA filler can be attributed to physical incompatibility; the spheres mixed poorly with the cement and separated quickly, floating to the top; combined with their bulky size (see Fig. 1), this created non-uniform, weak specimens that performed poorly in all temperatures. By comparison with specimens autoclaved at 200 °C, the hydrothermal treatment at 300 °C resulted in a loss of strength, with the rates of reduction in strength for DU- and MA-filled CPC specimens being lower than those for

TABLE II Properties of microspheres

Microsphere (symbol)	Density (g cm^{-3})	Particle size (μm)	Chemical composition of shell surfaces (wt%)								
			Si	Al	B	C	K	O	Fe	Ca	Na
Q-cel 650 (Q-C)	0.50	6–95	11.0	–	21.3	15.2	2.3	37.7	–	–	12.5
Extendospheres (EX)	0.67	75–200	13.1	10.1	–	37.8	2.0	36.5	–	–	0.5
Macrolite (MA)	1.25	300–450	6.4	19.7	–	30.8	1.8	36.8	2.3	–	2.2
Glass bubbles (GL)	0.38	5–45	11.6	–	16.9	25.7	2.4	31.7	–	1.9	9.8
Dualite (DU)	0.13	25–100	–	–	–	50.9	–	33.1	5.0	11.0	–

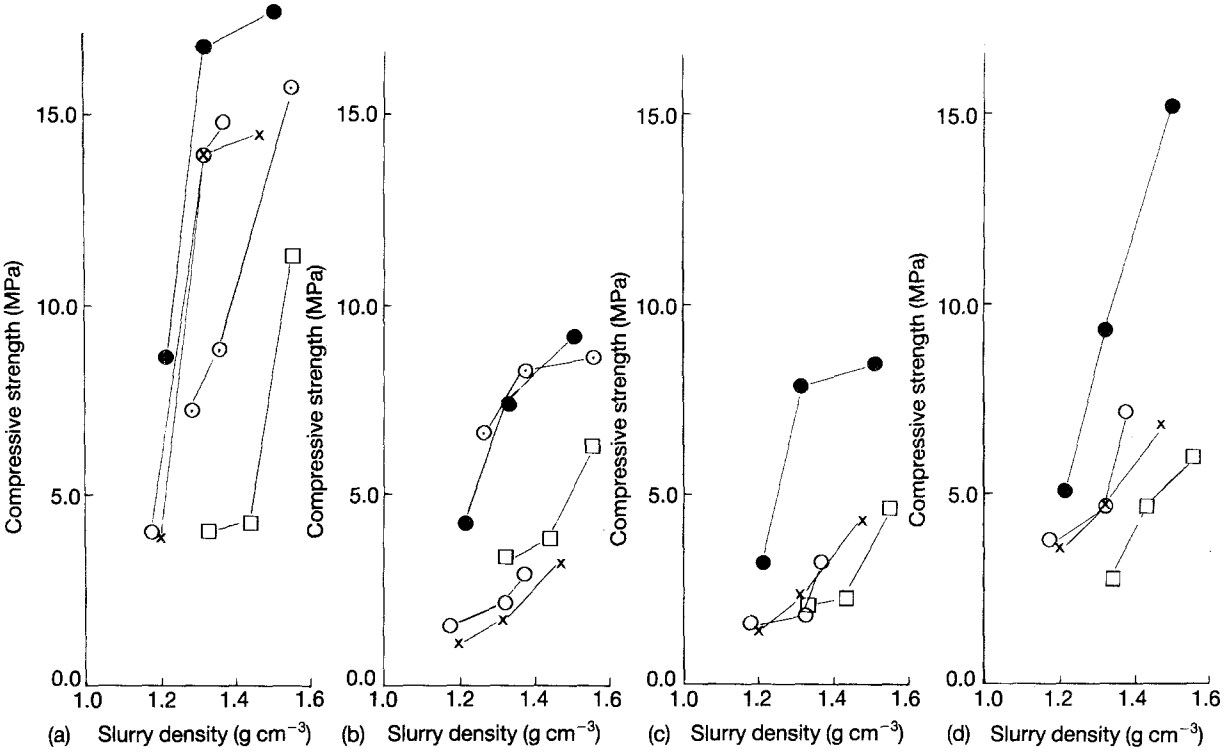

Figure 3 Compressive strengths of LCPC specimens as a function of slurry density: (a) 200 °C autoclaved, (b) 300 °C autoclaved, (c) 600 °C annealed and (d) 1000 °C annealed specimens. (○) Q-C, (●) EX, (□) MA, (×) GL, (⊙) DU.

the other microsphere-filled specimens. The mechanical strengths of the specimens made with the borosilicate-based glass fillers such as Q-C and GL were especially poor, exhibiting values between ≈1.0 and ≈3.0 MPa. When the 300 °C autoclaved specimens were heated in an oven to 600 °C, the strength–density relationships for the Q-C, EX and GL specimens differed little from those at 300 °C; while there was a slight reduction of strength in the MA specimens. In should be noted herewith that the strengths of the DU specimens to 600 °C were too low to be measured because a large number of shrinkage cracks developed in the LCPC. The 1000 °C annealing for all of the other specimens led to strengths greater than those at 300 and 600 °C. In particular, the EX specimens showed remarkable mechanical improvement.

3.3. Phase composition

To uncover the factors responsible for the losses and improvements in strength, efforts were concentrated on the phase compositions and transformations of LCPC specimens under hydrothermal and annealing conditions between 200 and 1000 °C, as determined by XRD and FTIR. XRD tracings, ranging from 0.371 to 0.249 nm, were made for 200 and 300 °C autoclaved Q-C, EX, MA, GL and DU specimens, including the 300 °C autoclaved specimens annealed at 600 and 1000 °C. CPC without microspheres served as the control. The results from these powder samples are given in Figs 4–7.

The diffraction patterns for all the 200 °C autoclaved specimens showed only non-reactive CA and CA_2 components from the No. 80 base reactant (Fig. 4). The calcite, $CaCO_3$, which was identified in the XRD pattern of DU-filled specimens (f), originated from the sizing material on the surface of the polymer shell. There were no d-spacings for reaction products between No. 80 and Poly-N, or for the shell materials of the microspheres. It was assumed then that the reaction products which bound the partially reacted and unreacted No. 80 particles into a coherent mass were amorphous phases. To identify the chemical make-up of this amorphous matrix, the 200 °C autoclaved untreated CPC specimens were investigated by FTIR (not shown), over the frequency ranges 100–800 cm^{-1}. A typical spectrum of the 200 °C specimens showed absorption bands at 1450 and 1410 cm^{-1}, which can be ascribed to NH_4^+ ions, and at 1100 and 1020 cm^{-1}, corresponding to stretching of the ionic P–O bond in $H_2PO_4^-$. Accordingly, a possible amorphous matrix derived from the acid–base reaction between the No. 80 powder as base reactant and the Poly-N solution as acid reactant at 200 °C is ammonium calcium orthophosphate (AmCOP) salt, $NH_4CaPO_4 \cdot xH_2O$ [7]. Since this acid–base reaction is caused by the uptake of Ca^{2+} by Poly-N, precipitating AmCOP, it is reasonable to believe that hydration of the Al oxides isolated from the Ca-depleted CA and CA_2 surfaces produces hydrous Al oxide gels, $Al_2O_3 \cdot xH_2O$.

The increase in autoclave temperature from 200 to 300 °C dramatically changed the features of the samples' diffraction patterns; several new spacings developed, although the residual CA and CA_2 related d-spacings remained (Fig. 5). The distinctive pattern of the untreated CPC specimen (b) revealed the formation of two new crystalline phases not present in the

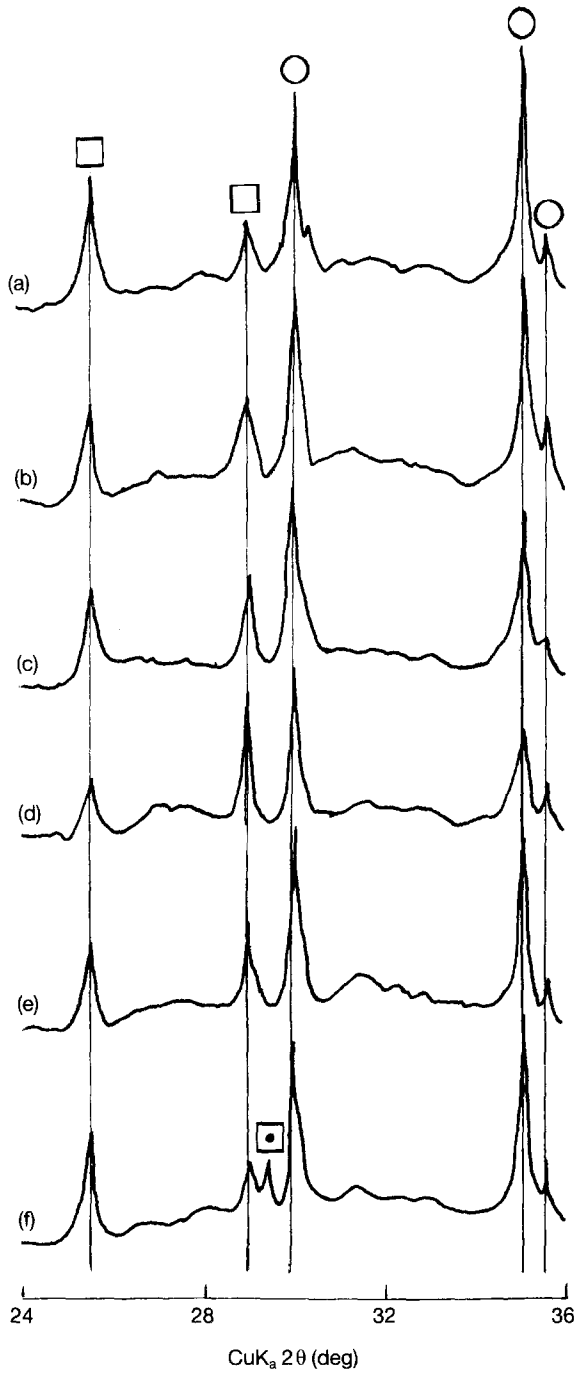

Figure 4 XRD patterns for 200 °C autoclaved LCPCs: (a) control, (b) Q-C, (c) EX, (d) MA, (e) GL and (f) DU cements. (○) CA, (□) CA_2, (□) $CaCO_3$.

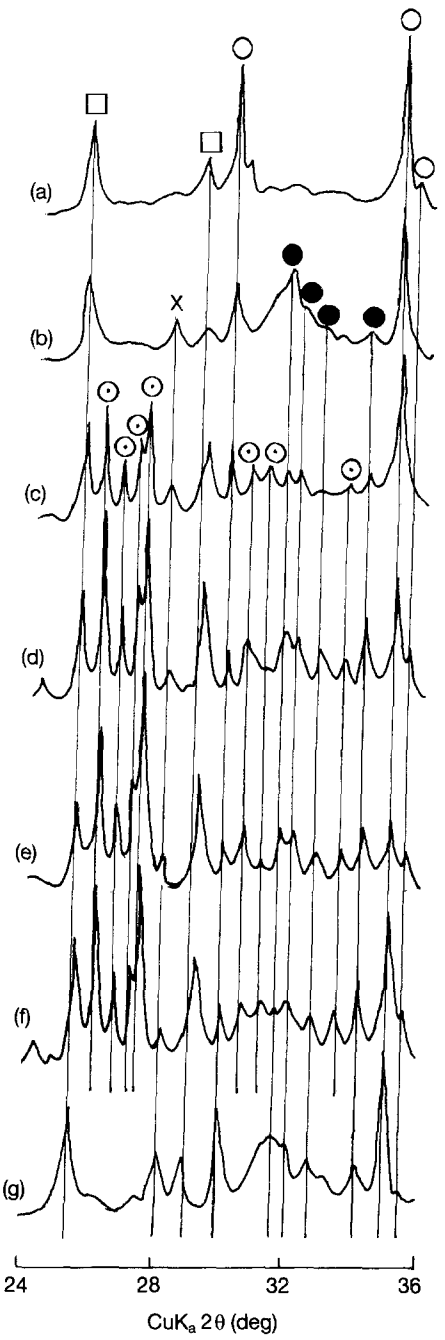

Figure 5 XRD patterns for (a) 200 °C autoclaved control CPC and 300 °C autoclaved, (b) control, (c) Q-C, (d) EX, (e) MA, (f) GL and (g) DU specimens. (○) CA, (□) CA_2, (●) $Ca_5(PO_4)_3(OH)$, (×) γ-AlOOH, (⊙) $(Ca_{2.6}Na_{1.1}K_{0.1})(Al_{6.3}Si_{17.7})O_{48}\cdot 16H_2O$.

200 °C autoclaved CPC (a), hydroxyapatite (HOAp), $Ca_5(PO_4)_3(OH)$, and boehmite (BO), γ-AlOOH. HOAp and BO may have been formed by phase transformations of AmCOP salt and $Al_2O_3\cdot xH_2O$ gels, respectively. Detailed information on these *in situ* AmCOP → HOAp and $Al_2O_3\cdot xH_2O$ → BO phase transitions was reported in a previous paper [7]. Due to the conversions which occurred in the untreated CPCs, considerable attention was paid to XRD results from the various LCPC specimens. An interesting pattern produced by the Q-C (c), EX (d), MA (e), and GL (f) specimens reflected the addition of a new phase among the non-reactive CA and CA_2, HOAp and BO hybrid phases. This new phase was epistilbite (EP), $(Ca_{2.6}Na_{1.1}K_{0.1})(Al_{6.3}Si_{17.7})O_{48}\cdot 16H_2O$, which can be classified as a calcium aluminate silicate hydrate species. The formation of EP strongly suggested that under hydrothermal environments at 300 °C, the Si, Na and K in the shell structure of the microspheres preferentially reacted with unreacted CA or CA_2, rather than with Poly-N. In fact, for these LCPCs, the intensity of the HOAp related lines, which identify the reaction product of CA or CA_2 with Poly-N, was relatively weaker than that of the neat CPC, indicating a tendency for CA and CA_2 to react with the microspheres instead of with Poly-N. The differences in the intensity of the HOAp line among the LCPCs showed that the degree of HOAp crystallinity depends primarily on the chemical components of the filler; borosilicate based glass microspheres such as Q-C (c) and

GL (f) resulted in poor formation of HOAp. In contrast, well crystallized HOAp was achieved through the incorporation of aluminosilicate and nepheline syenite based microspheres such as EX (d) and MA (e) into the CPC. As expected, no EP formation was found on the XRD pattern of the Si, K and Na free DU polymer-filled CPC (g). However, the DU samples displayed strong line intensities indicative of well formed HOAp and BO.

At 600 °C (Fig. 6), the spacing pattern of CPC alone (a) was similar to that of the 300 °C autoclaved CPC (Fig. 5b), except for the loss of the BO related line. It is uncertain whether this disappearance was due to the thermal decomposition of BO or the phase transformation of BO into other aluminium compounds. The patterns for the borosilicate microsphere-filled specimens (b) and (e) were interesting; two new phases appeared, whitlockite (WH), β-$Ca_3(PO_4)_2$ and anorthite (AN), $CaAl_2Si_2O_8$, while the line signals of HOAp and EP were considerably attenuated or had vanished. The coincident disappearance of EP and HOAp and formation of AN and WH at 600 °C may have been due to $(Ca_{2.6}Na_{1.1}K_{0.1})(Al_{6.3}Si_{17.7})O_{48}\cdot 16H_2O \rightarrow CaAl_2Si_2O_8$, and $Ca_5(PO_4)_3(OH) \rightarrow$ β-$Ca_3(PO_4)_2$ phase transitions. Although such hydrate → anhydrate phase conversions were observed in

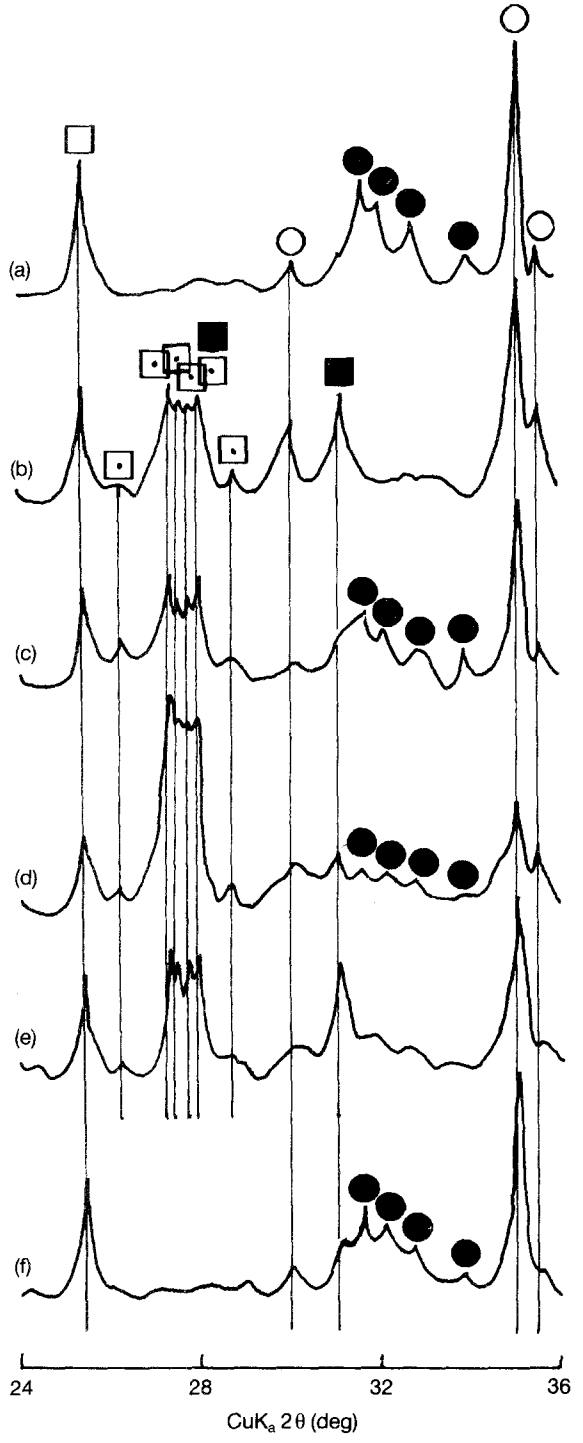

Figure 6 XRD patterns for 600 °C annealed (a) control, (b) Q-C, (c) EX, (d) MA, (e) GL and (f) DU specimens. (○) CA, (□) CA_2, (●) $Ca_5(PO_4)_3(OH)$, (⊡) $CaAl_2Si_2O_8$, (■) β-$Ca_3(PO_4)_2$.

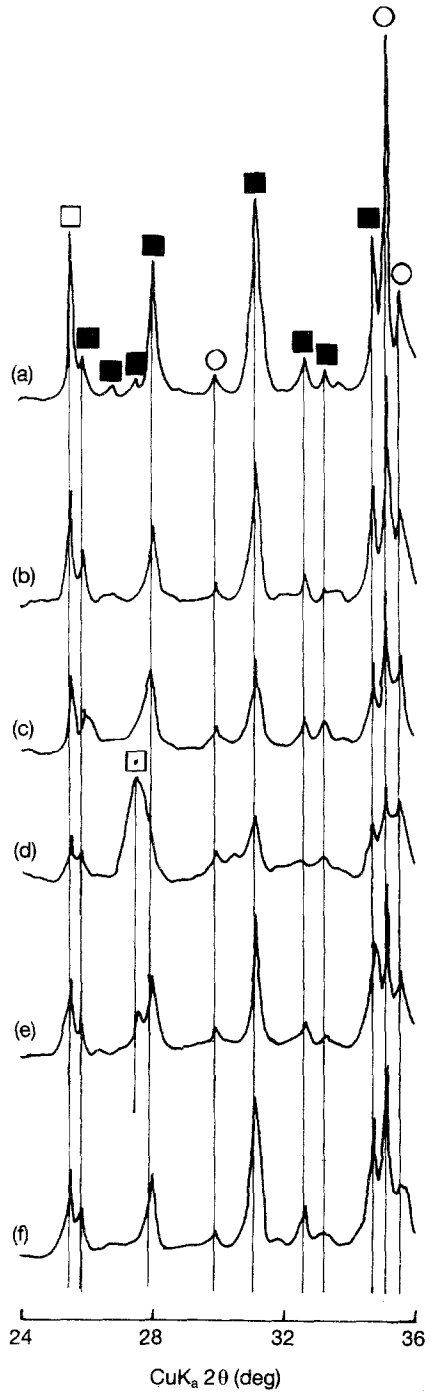

Figure 7 XRD patterns for 1000 °C annealed (a) control, (b) Q-C, (c) EX, (d) MA, (e) GL and (f) DU specimens. (○) CA, (□) CA_2, (⊡) $CaAl_2Si_2O_8$, (■) β-$Ca_3(PO_4)_2$.

the patterns of EX (c) and MA (d) LCPCs, these specimens also maintained weak peaks identifying HOAp. The pattern of the DU specimen (f) closely resembled that of CPC alone (a).

The further increase in temperature to 1000 °C for the CPC (a), Q-C (b), EX (c) and DU (f) specimens led to the formation of a WH phase as the single reaction product, with no AN phase (Fig. 7). However, the XRD data demonstrated that some AN still remained in the MA (d) and GL (e) specimens. Thus, AN appears to thermally decompose between 600 to 1000 °C.

To relate these phase-related assessments to the compressive strengths of the LCPC specimens, attention was focused on understanding the phase assemblages and transformations governing the improvement and retrogression of compressive strength as a function of temperature. The interpretation of these findings is as follows. For all LCPC specimens autoclaved at 200 °C, the amorphous AmCOP salt was responsible for the development of compressive strength. For specimens autoclaved at 300 °C, the loss in strength was accompanied by the formation of an EP phase by hydrothermal interaction between CA or CA_2 in the No. 80 reactant and the microspheres containing Si, Na and K, and also by the phase transformation of amorphous AmCOP to crystalline HOAp in conjunction with the $Al_2O_3 \cdot xH_2O$ gels → crystalline BO phase transition. Although excessive *in situ* growth of crystalline phases in the amorphous matrices causes strength to retrogress, high rates of reduction are more likely to be related to the structural interference of well formed EP, rather than crystals of HOAp and BO. This conclusion is supported by the severe temperature-related strength losses in the GL and Q-C samples, which did not form as much HOAp phase as the other LCPCs. The phase conversions of EP and HOAp into AN and WH, respectively, and the elimination of the BO phase occurred at 600 °C; however, there were no significant changes in compressive strengths. Despite the continued presence of HOAp, the serious loss of strength for DU-filled specimens was probably related directly to thermal decomposition of the polymer microspheres incorporated into the CPC matrices. At 1000 °C, the HOAp → WH phase transition and the considerable reduction of AN layers contributed to an increase in strength above those of the 600 °C annealed specimens.

3.4. Microstructural development at microsphere–CPC interfaces

Several questions which cannot be resolved by XRD and i. r. analysis still remain. The following need to be determined:

1. how the bond formations and structures at the interface between the CPC matrix and microsphere filler relate to strong or weak mechanical behaviours,
2. how the microspheres incorporated into the CPC are susceptible to thermal and hydrothermal degradations, and
3. why the aluminosilicate based microspheres denoted as EX contribute more than other microspheres to the gain in strength of the 1000 °C annealed specimens. To obtain this information, a combination of SEM image and EDX elemental analyses at LCPC compressive strength failure surfaces were undertaken. Three LCPCs, Q-C, EX and DU specimens, were employed in this study.

Figs 8 and 9 show the SEM micrographs coupled with the EDX inspections of the fractured surfaces of the 200 and 300 °C autoclaved Q-C filled LCPC specimens. The SEM image of the 200 °C autoclaved specimen (Fig. 8) revealed that failure occurred through two different modes, one of which was an adhesive mode in which separation occurred at the critical

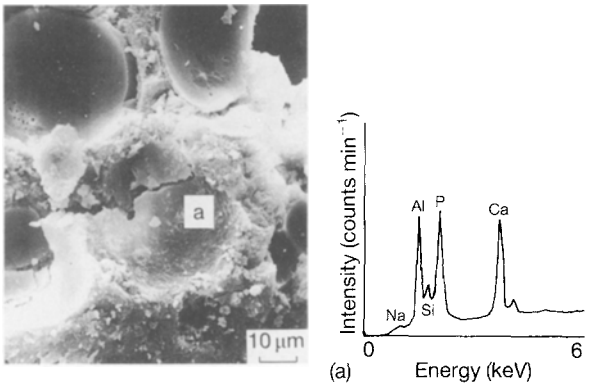

Figure 8 SEM–EDX analysis of the fracture surface of a 200 °C autoclaved Q-C specimen.

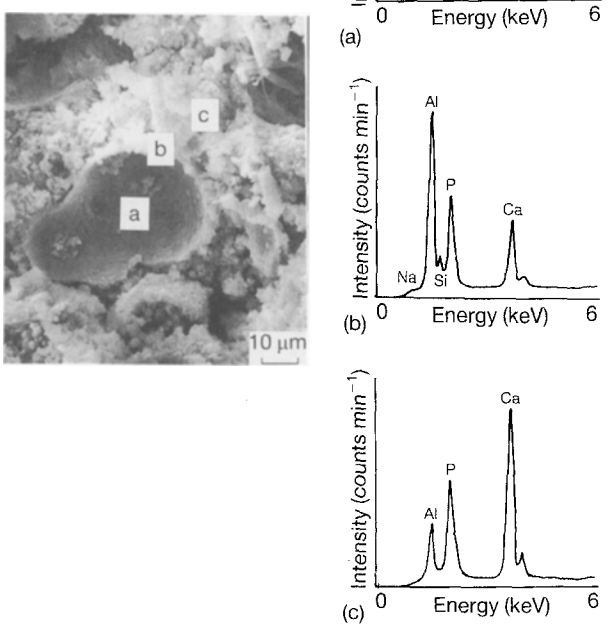

Figure 9 SEM image of the fracture surface of a 300 °C autoclaved Q-C. EDX analyses of (a) inner microsphere surface, (b) interfacial compound and (c) cement matrix.

boundary regions between the CPC and Q-C microsphere, leaving either matrix craters or smooth microspheres without any CPC coverage on the fractured matrix surface. The other mode of failure was a cohesive one, occurring through the microsphere shell. This mode was demonstrated by the pieces of microsphere left from the partial breakage of the shell surfaces. Such a mixture of adhesive and cohesive failures suggested that there was moderate interfacial bonding of the microsphere–matrix in the 200 °C autoclaved Q-C LCPCs. EDX inspection of the area denoted as location "a" in the matrix crater identified Ca, P and Al as the major chemical components, with smaller amounts of Na and Si. Since the minor elements originated from the Q-C microspheres and the major elements corresponded to the CPC matrix, it was apparent that some Na and Si from the Q-C shells remained on the matrix sites after failure. This observation suggested that the surfaces of the Q-C microspheres partially reacted with the CPC in the autoclave at 200 °C. The resulting intermediate reaction product was probably weaker than the microsphere itself, causing frequent failure in the layers adjacent to the sphere. It was noted that the microsphere element B cannot be detected by EDX, because its emission energy (keV) is too low.

The interfacial bond formed by the 300 °C hydrothermally catalysed interaction between the Q-C microsphere and CPC (Fig. 9) was also examined. An EDX spectrum similar to the 200 °C plot was collected inside the matrix depression at site "a". EDX data for matrix site "b" at the depression's edge identified a strong presence of Al. Since the only Al source was the matrix, a large amount of Al apparently migrated onto the microsphere's surface. It is believed that the Al-rich areas surrounding the crater were related directly to the formation of intermediate layers produced by Q-C–CPC interaction. Although this reaction product contains P, the other elements may identify the formation of an EP phase. The intermediate layer perhaps promoted cross-linking and coupling which tightly connected the microsphere to the CPC. The locus of bond failure between the CPC and Q-C may be in the intermediate reaction product layers. As opposed to the SEM image of the 200 °C specimen, the 300 °C micrograph and EDX of the CPC matrix (site "c") displays a growth of fine needle-like crystals containing Ca, P and Al within the amorphous phase. These elements may reveal the formation of HOAp and BO crystals, whose *in situ* growth seems to produce a porous microstructure.

Fig. 10 illustrates the SEM–EDX results in the interfacial region of a fracture surface of a 200 °C autoclaved EX microsphere-filled LCPC specimen. The recessed microsphere fractured through its shell, as is evident by the smooth surface of the shell thickness. A low magnification view of the EX fracture surface (not shown) confirmed that such cohesive failure was common, although interfacial adhesive failure also occurred. The sharpness of the microsphere–matrix interface suggested that this adhesive failure was due to a lack of EX–CPC chemical interaction and consolidation. An EDX analysis

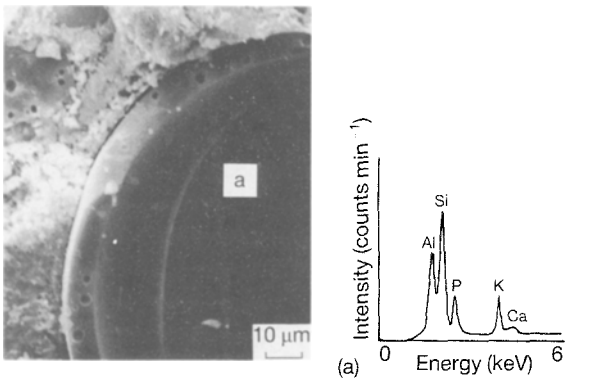

Figure 10 SEM–EDX analysis of the fracture surface of a 200 °C autoclaved EX specimen.

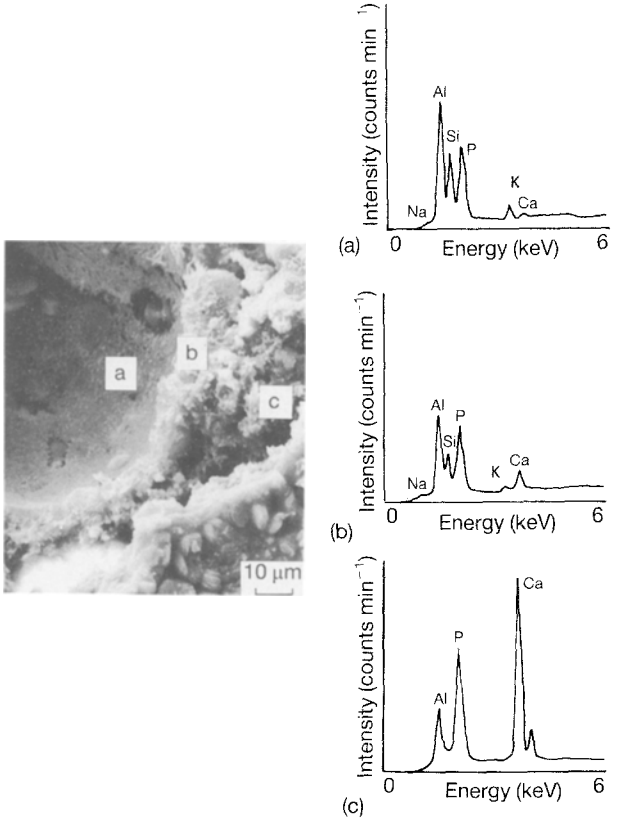

Figure 11 SEM image of the fracture surface of a 300 °C autoclaved EX. EDX analyses of (a) inner microsphere surface, (b) interfacial area and (c) cement matrix.

of the inner microsphere surface, with strong Al and Si peaks, moderate K and P peaks, and a minimal Ca peak, strongly supported this assertion. The weakness of the peak intensity of Ca, a matrix-related element, suggested that there was little ion exchange between microsphere and matrix. The higher P peak may be due to ion migration or to the penetration of Poly-N solution into the shell during preparation of the cement.

Fig. 11 shows the microstructure of the fracture surface of the 300 °C autoclaved EX specimen. The EDX sites "a", "b" and "c" are located on the depression wall, the intermediate layer formed by interaction between microsphere and matrix, and the matrix, respectively. The dense amorphous structure of the

200 °C matrix was transformed into a more porous structure because of the *in situ* growth of crystalline species at 300 °C such as HOAp and BO. The EDX spectrum at site "a" on the depression wall was characterized by strong Al, Si and P signals, weaker K peaks, and negligible signs of Na and Ca. The Al and Si elements can be ascribed to the residual parts of an aluminosilicate shell. There is no evidence whether the presence of P is due to penetration of Poly-N, as speculated earlier, or related to a P-incorporated Al_2O_3–SiO_2 reaction product. The increase in the signal intensity of Ca on the EDX data at site "b" in the intermediate layers suggested that migration of Ca from the CPC to the microsphere surfaces may create the EP interfacial reaction product. Nevertheless, the remnants of microsphere shells in the matrix, identified by the EDX tracing, suggest that the major failure mechanism is cohesive, occurring through the microsphere shell.

From this information on failures and microstructure developments at Q-C and EX–CPC interfaces, a possible interpretation for the loss in strength of 300 °C autoclaved specimens is proposed; the strong chemical affinity between the microsphere's surfaces and CPC not only led to the formation of intermediate layers, which improved the interfacial bond strength between them, but also decreased the effective thickness of the hollow microsphere shell. The latter effect might cause the distribution of mechanically weak microspheres in the matrix phases. Since cohesive failure of the microsphere was observed in all four fracture surfaces, the retrogression of strength may be related to the high extent of microsphere–CPC interaction, rather than to the development of a porous microstructure brought about by the *in situ* conversion of amorphous AmCOP and $Al_2O_3 \cdot xH_2O$ into crystalline HOAp and BO, respectively.

Fig. 12 shows the SEM–EDX examinations for 200 °C (top) and 300 °C (bottom) autoclaved DU-filled LCPC specimens. At 200 °C, the crater wall has a peculiar sponge-shaped, foamy liner whose thickness was roughly 15 μm (denoted as site "a"). As seen in the EDX data, this porous rim consists of Ca, P and Al. Assuming that the rim was formed by interactions between the CPC and $CaCO_3$ DU coating, failure at the sphere–matrix interface could have been due to internal stresses generated by the formation of this reaction product between the polymer microsphere and matrix. The image also suggested that such internal stress could lead to the development of cracks between the porous rim and matrix.

A striking difference in microstructure was observed on the fracture surface of the 300 °C DU specimen. A distinctive interlocking structure of well formed plate-like crystals containing Ca, P and Al dominated the inside of the crater. The formation of this phase indicated that hydrothermal treatment at 300 °C converted the sponge-like lining into a well crystallized rim. Further, no microspheres were visible on the fracture surface at this temperature, implying that hydrothermal decomposition of the polymeric microspheres occurred between 200 and 300 °C. This decomposition might cause the development of microcracks in the cement body, partially accounting for the losses in strength exhibited by DU specimens treated at and above 300 °C. More importantly, the lack of a solid DU aggregate in the 600 and 1000 °C annealed specimens allowed shrinkage of the matrix, apparent in the reduced size of annealed specimens, to extensively crack and weaken the specimens.

Fig. 13 is the SEM image of a 1000 °C annealed Q-C specimen. The 5–20 μm gaps in the microstructure, and the disappearance of the microspheres, clearly document that the borosilicate based microspheres had thermally decomposed below this temperature. The EDX analysis at site "a" on the matrix recognized Ca and P as the dominant chemical components, with lesser amounts of Al and Si. The minor elements may have been the remains of the pyrolysed AN phase,

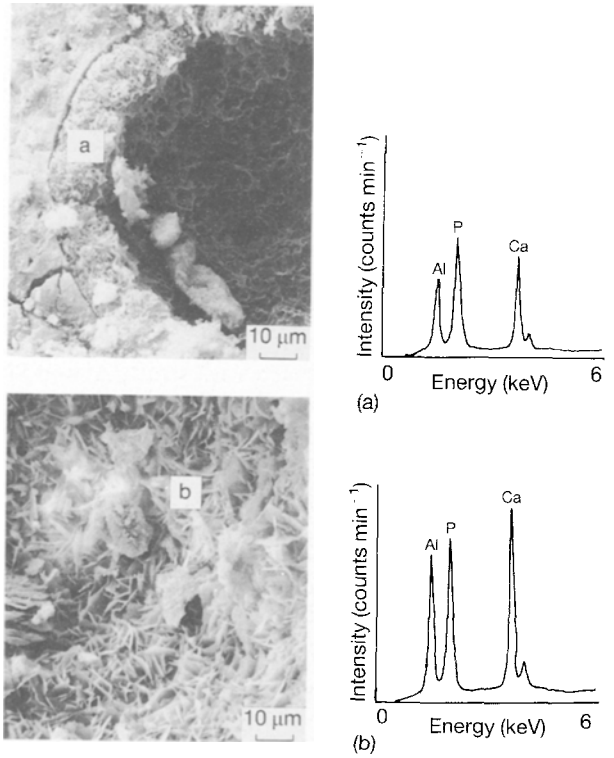

Figure 12 SEM–EDX analyses of the microsphere–matrix interface of (a) 200 and (b) 300 °C autoclaved DU specimen.

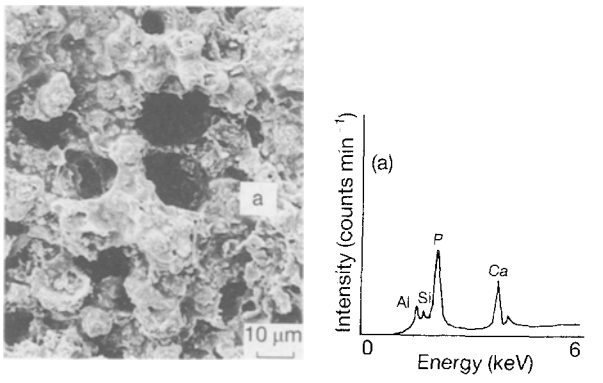

Figure 13 SEM–EDX analysis of the fracture surface of a 1000 °C annealed Q-C specimen.

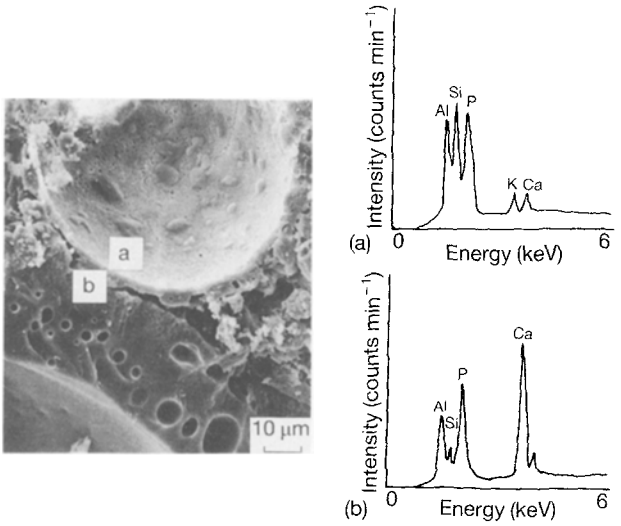

Figure 14 SEM image of the fracture surfaces of a 1000 °C annealed EX specimens. EDX analyses of (a) inner microsphere surface and (b) microsphere–matrix interface.

which was derived from EP at 600 °C. The Ca and P most likely corresponded to WH. The $Ca_5(PO_4)_3(OH) \rightarrow \beta\text{-}Ca_3(PO_4)_2$ phase transition at 1000 °C probably was responsible for the improvement in strength over the 300 °C specimens. Although the new matrix was wrought with large gaps, it appeared to be much denser than the 300 °C microstructure.

The SEM–EDX results from a 1000 °C annealed EX specimen are shown in Fig. 14. The existence of recessed shells suggested that the EX microspheres remained in the cement and failure occurred through the shell. The EDX at site "a", on the inner surface of a microsphere, indicated the presence of EX components Al, Si and K, but also revealed the matrix elements P and Ca. Close examination of the image shows that the shell thickness was severely reduced to ≈ 3 μm, allowing the EDX electron to penetrate to the matrix directly below the microsphere and identify P and Ca. The reduction in thickness of the microsphere and the obscurity of the microsphere–matrix interface suggest that some EX–CPC interaction occurs at 1000 °C. The EDX spectrum at the matrix adjacent to the microsphere, site "b", was characterized by strong Ca and P line intensities, moderate Al intensity and a weak Si signal. The presence of Al and Si peaks in this region attested to the remains of microsphere–matrix reaction products, while the Ca and P probably composed WH. The matrix resembled the 1000 °C Q-C matrix (Fig. 13), but with its EX microspheres intact contrasted with the skeletal Q-C microstructure. This new, denser matrix phase, combined with the high temperature stability of the EX microsphere, resulted in the significant gain in strength of the EX microsphere-filled LCPC specimen at 1000 °C.

4. Conclusions

Lightweight calcium phosphate cement (LCPC) slurries were prepared by incorporating four inorganic microspheres, borosilicate based glasses (Q-C and GL), aluminosilicate (EX), nepheline syenite (MA) and a $CaCO_3$ sized acrylonitrile copolymer organic microsphere (DU), into calcium phosphate pastes derived from calcium aluminate cement as base reactant with an $NH_4H_2PO_4$ based fertilizer (Poly-N) as acid reactant. The densities of these LCPC slurries ranged from 1.55 to 1.18 g cm^{-3}, while the neat calcium phosphate cement (CPC) paste had a density of 1.98 g cm^{-3}. These LCPC slurries were autoclaved at 200 and 300 °C, and additional 300 °C autoclaved specimens were oven-annealed in air at 600 and 1000 °C. Although cement density directly affected the LCPC compressive strengths at all temperatures, it was found that the following important factors governed the development and loss of strength:

1. phase composition and transformation of the matrix itself and the interfacial reaction product formed by interactions between the microspheres and the CPC,
2. changes in microstructure developed at the microsphere–CPC interfaces and in the matrix phase, and
3. susceptibility of the microspheres to hydrothermal and thermal decompositions.

After autoclaving at 200 °C, the formation of amorphous ammonium calcium orthophosphate (AmCOP) salt, $NH_4CaPO_4 \cdot xH_2O$, and aluminium oxide gel, $Al_2O_3 \cdot xH_2O$, as matrix phases which bind the non-reactive No. 80 particles into a coherent mass, was primarily responsible for the development of compressive strength. Based upon a mean slurry density of ≈ 1.3 g cm^{-3}, the compressive strengths of the microsphere-filled cements decreased in the following order: EX > Q-C = GL > DU > MA. The MA LCPC specimens exhibited poor strength at every temperature due to the separation of the microspheres from the cement phase in the slurries.

The 300 °C autoclaved AmCOP and $Al_2O_3 \cdot xH_2O$ compounds were transformed into crystalline hydroxyapatite (HOAp), $Ca_5(PO_4)_3(OH)$ and boehmite (BO), γ-AlOOH, phases, respectively. However, the degree of crystallinity of HOAp and BO depended primarily on the chemical components of the microsphere shells; Q-C and GL-filled LCPC specimens produced few HOAp and BO crystals. Microspheres containing Si, Na and K favourably reacted with the CPC matrix at 300 °C, forming epistilbite (EP), $(Ca_{2.6}Na_{1.1}K_{0.1})(Al_{6.3}Si_{17.7})O_{48} \cdot xH_2O$, as an intermediate reaction product. In contrast, interaction between the $CaCO_3$ sized polymeric DU microsphere and the CPC at this temperature produced an intermediate reaction product rim of well formed, thin plate-like crystals consisting of Ca, P and Al. Even though the formation of these intermediate layers in the critical interfacial regions cross-linked and coupled the microspheres to matrix, the high reactivity of the microsphere shell and CPC may have mechanically weakened the microsphere shell. Assuming that this concept is correct, the losses in strength of the 300 °C autoclaved specimens were more likely related to the extensive production of EP phase and subsequent reduction of microsphere shell thickness, rather than to a porous structure created by HOAp and BO formation in the dense

amorphous AmCOP phases. The reactivity of the borosilicate based glass shells was much greater than those of other shells, thereby resulting in larger reductions in strength in Q-C and GL LCPCs between 200 and 300 °C.

Annealing at 600 °C prompted the EP → anorthite (AN), $CaAl_2Si_2O_8$, phase transition for all of LCPC specimens, except for the DU-filled specimen, and eliminated the BO phase. All of the HOAp in the Q-C and GL specimens was completely converted into whitlockite (WH), β-$Ca_3(PO_4)_2$. In contrast, this $Ca_5(PO_4)_3(OH) \rightarrow \beta$-$Ca_3(PO_4)_2$ phase transition progressed to a far lesser extent in the EX, MA and DU specimens. However, amidst all these transformations, there were no significant changes in strength. As expected, the thermal disintegration of DU microspheres within the CPC occurred before 600 °C, thereby resulting in a severe loss in strength.

The phase transformation of HOAp into WH was completed between 600 and 1000 °C, while none of the microsphere–CPC reaction product AN remained. The excellent thermal stability of the EX microspheres in conjunction with the formation of the WH phase led to the increase in strength of its 1000 °C annealed LCPCs. The pyrolysis of the borosilicate based glass microspheres at 1000 °C allowed WH formation to yield only modest strength gains in the Q-C and GL specimens.

Based on its consistent enhancement in strength and high temperature stability, it is believed that the aluminosilicate based hollow microspheres have a high potential for use as lightweight filler in calcium phosphate cementitious material systems, under hydrothermal and annealing conditions between 200 and 1000 °C.

Acknowledgements

Eric Wetzel acknowledges support from the Department of Energy's Division of University and Industry Programs, Office of Energy Research, as a Science and Engineering Research Semester (SERS) Program participant.

References

1. T. SUGAMA, G. GRAY and L. E. KUKACKA, *J. Mater. Sci.* **27** (1992) 180.
2. T. SUGAMA, N. R. CARCIELLO and G. GRAY, *ibid.* **27** (1992) 4909.
3. *Idem, J. Amer. Ceram. Soc.* **74** (1991) 1023.
4. *Idem, Adv. Cem. Res.* **5** (1993) 31.
5. T. SUGAMA and N. R. CARCIELLO, *Cem. Concr. Res.* **22** (1992) 783.
6. T. SUGAMA, L. E. KUKACKA, B. G. GALEN and K. WOO, *J. Mater. Sci.* **22** (1987) 4313.
7. T. SUGAMA, M. ALLAN and J. M. HILL, *J. Amer. Ceram. Soc.* **74** (1992) 2076.
8. T. KOKUBO, S. YOSHIHARA, N. NISHIMURA and T. YAMAMURA, *ibid.* **74** (1991) 1739.

Received 7 January 1993
and accepted 21 March 1994